

Multi-Functionalization Integration into the Electrospun Nanofibers Exhibiting Effective Iodine Capture from Water

Dingyang Chen,[#] Tingting Ma,[#] Xinyue Zhao, Xiaofei Jing, Rui Zhao,* and Guangshan Zhu



Cite This: *ACS Appl. Mater. Interfaces* 2022, 14, 47126–47135



Read Online

ACCESS |

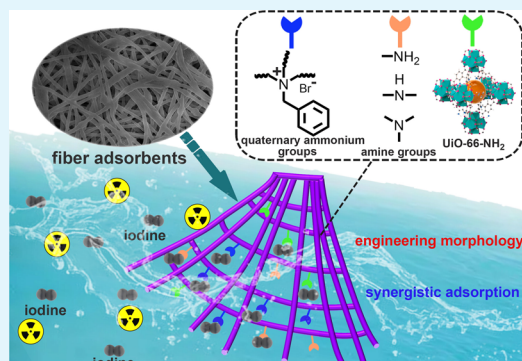
Metrics & More

Article Recommendations

Supporting Information

ABSTRACT: Efficient capture of radioiodine from aqueous solutions is of importance for sustainable development of nuclear energy and protection of the environment. However, current adsorbents under exploration suffer from limited adsorption capacity and powder form that are unfavorable for practical applications. Herein, we applied a “multi-functionalization integration” idea to construct novel electrospun fiber adsorbents (N-MOF-PAN fibers) containing cationic quaternary ammonium groups, uncharged amine groups, and porous MOF material ($\text{UiO}-66-\text{NH}_2$), which in synergy adsorb iodine effectively from both saturated I_2 aqueous solution and I_3^- aqueous solution. Iodine species (94.6%) could be removed from saturated I_2 solution within 180 min, and 98.7% of iodine species were captured from I_3^- solution within 240 min. Additionally, the N-MOF-PAN fibers exhibited high iodine uptake capacities of 3.56 g g^{-1} from a concentrated KI/I_2 aqueous solution and 3.61 g g^{-1} from the Langmuir isotherm model, surpassing many reported iodine adsorbents in the aqueous medium. Characterization and mechanism analysis indicated that multiple active sites simultaneously attribute to the high binding affinity toward iodine species through physical adsorption and chemical adsorption. Furthermore, benefiting from their macroscopic architecture, N-MOF-PAN fibers were used as the adsorption column for dynamic iodine capture with a bed volume of 1490 mL, which is much higher than commercially activated carbons. Overall, this work provides guidance for the development of novel fiber adsorbents for related applications.

KEYWORDS: *electrospinning, fiber adsorbents, iodine capture, N-containing functional groups, $\text{UiO}-66-\text{NH}_2$*



1. INTRODUCTION

Currently, nuclear energy is making tremendous contributions to the sustainable development of modern society but simultaneously producing massive radioactive wastes, which emerge as an enormous challenge toward the environment and public health.^{1,2} Radioactive iodine isotopes (e.g., ^{131}I or ^{129}I) generated by uranium fission are one of the most hazardous pollutants in nuclear disposal and accidents owing to the extremely large half-life (1.6×10^7 years) of ^{129}I , high volatility and biotoxicity, strong radiation, easy aggregation in glands, and so on.^{3,4} If not appropriately solved, the release of radioiodine will seriously cause adverse effects on air and water. Accordingly, the demand for efficiently reprocessing of iodine isotopes from nuclear fuel becomes more and more urgent.⁵ In recent years, a great majority of studies have concentrated on the recovery of iodine from the gaseous phase or organic solvents, while few studies of iodine adsorption from aqueous solution are conducted but equally significant.^{6,7} This is because the cooling process of nuclear fission reactors is mainly water cooling, leading to a direct radioactive iodine release in water. In addition, radioactive iodine used in medical cancer diagnosis and therapy is also the wastewater discharge

source.^{8,9} Thus, an in-depth research about radioactive iodine removal from water is necessary and has certain importance.

Solid-phase adsorption is considered as an effective approach to capture radioiodine in nuclear waste reprocessing.¹⁰ At present, the most widely studied iodine adsorbents are advanced porous materials including metal–organic frameworks (MOFs), covalent organic frameworks (COFs), porous aromatic frameworks (PAFs), and other porous organic polymers.^{11–13} They have shown great potential for the capture of gaseous radioactive iodine because of their high surface areas and tunable pore structures. However, the powder form of advanced porous materials limits their extensive use in iodine adsorption from the aqueous medium in considering the recyclability, stability, and scalability. Macroscopic polymeric fibers have been widely applied as adsorbents for sewage disposal on account of their large-scale

Received: August 16, 2022

Accepted: September 27, 2022

Published: October 6, 2022



preparation, satisfying mechanical property, and low cost.^{14,15} Electrospinning technology, as a burgeoning nano/microfiber manufacturing process, which produces continuous fibers under high electrostatic force conditions, shows the unique advantages in versatility, flexibility, convenient preparation, highly accessible active sites, and easy regeneration.¹⁶ Based on the above fascinating characteristics, electrospun fibers are efficient adsorbents to remove various contaminants from water.^{17–19} However, there are few examples of electrospun fibers that are explored for radioiodine elimination.²⁰ Consequently, it is urgent to develop electrospun fibrous iodine adsorbents with high efficiency and potential for practical applications. Nevertheless, some defects still exist in traditional electrospun fiber materials that tremendously impede the radioactive iodine trapping.

Apparently, weak interactions exist between electrospun fibers and the captured iodine molecules, leading to a low adsorption ability. The captured iodine through physical adsorption is also released easily when immersed in organic solvents, which is unfavorable for the long-term storage of iodine.²¹ Extensive research into iodine capture has found that nitrogen-containing structures could facilitate the high iodine uptake of host materials. He and co-workers fabricated nitrogen-rich porous organic polyaminals by the condensation reaction from N-containing monomers. The N sites with high electron density offered the host–guest interactions making the polyaminals display a high iodine capture capacity of 3.58 g g⁻¹ in the vapor phase.²² Azambre's group impregnated branched polyethyleneimine into nanosilica adsorbents, and the results demonstrated that the adsorption iodine capacities depend on the N content of the samples.²³ Additionally, studies showed that cationic adsorption sites could also promote the iodine adsorption to capture the formed polyiodide anions by Coulomb interactions.²⁴ Han's group constructed ionic covalent organic frameworks, and Ghosh's group prepared ionic porous organic polymers.^{7,25} They both found that cationic binding sites are beneficial to iodine capture. Another crucial problem is that the continuous electrospun fibers have a limited specific surface area, which further restricts the I₂ capture. To solve this issue, the introduction of advanced porous materials such as MOFs, COFs, PAFs, etc., into polymer matrices to capture specific ions or molecules has become a research hotspot recently,^{26–28} which is also an effective strategy to enhance the adsorption ability of the polymer host. Thus, to extend the application scope of fiber materials in tackling the problem of radioactive iodine in water, the rational design and synthesis of electrospun fibers that integrate the specific adsorption sites and porous materials are of great significance for both material and environment science.

In this work, we reported a stable and recyclable electrospun fiber adsorbent with multiple binding sites including N-containing functional groups (cationic quaternary ammonium and uncharged amines) and porous materials (UiO-66-NH₂) that are prepared from blending electrospinning and the following functionalization reactions. Branched polyethyleneimine (PEI) with abundant amine groups (–NH₂, –NH–, and –N<) was used to construct the N-containing functional groups in the fibers. After the quaternization reaction, the tertiary amines could be also converted into quaternary ammonium groups to obtain cationic binding sites. The MOFs of UiO-66-NH₂ were selected as the porous material additive because of its good stability, high specific surface area,

and simple synthesis.²⁹ The adsorption performance of the as-prepared fiber adsorbents toward iodine from aqueous media was studied in static adsorption and dynamic column adsorption, which both receive effective iodine capture performance. The adsorption capacity comparison and adsorption mechanism investigation demonstrated that cationic quaternary ammonium groups, uncharged amine groups, and porous materials synergistically attributed to the iodine adsorption involving chemisorption and physical adsorption.

2. EXPERIMENTAL SECTION

2.1. Materials. Zirconium chloride and 2-aminoterephthalic acid were purchased from Aladdin. Polyacrylonitrile (PAN, M_w = 150, 000) was obtained from Shanghai Macklin Biochemical Co., Ltd. Branched polyethyleneimine (PEI, M_w = 600), benzyl bromide (98%), I₂ (AR), and glutaraldehyde (50%) were purchased from Aladdin. The inorganic salts were purchased from Beijing Chemical Factory. All other chemicals and reagents were used as received without further purification.

2.2. Procedure for the Synthesis of Fiber Adsorbents. UiO-66-NH₂ was synthetized according to the literature with slight modification,³⁰ and its synthesis process is shown in the *Supporting Information*. To prepare the fiber materials, polyacrylonitrile (PAN, 8.16 g) was dissolved in N,N-dimethylformamide (DMF, 75 mL) in a round bottom flask stirring at 85 °C for 12 h and the obtained PAN solution (wt = 10%) was cooled to room temperature. Then, 10 g of PAN solution, 2 g of PEI, and 2 g of UiO-66-NH₂ powder were placed in a 20 mL cylindrical glass bottle stirring at 25 °C for 36 h. The resulting mixture was poured into a 20 mL dry syringe and then was electrospun into continuous fibers on a flat plate under high-voltage static electricity. The obtained fibers were chemically cross-linked in glutaraldehyde (wt = 30%) vapor. After the cross-linking reaction for 12 h, the fibers were washed with deionized water and ethanol three times, dried in vacuum at 70 °C, and sealed for storage. The cross-linked fibers (30 mg) were reacted with benzyl bromide (1 mL) in 20 mL of ethanol at 85 °C for 8 h. After ultrasonic cleaning, the product was washed twice with ethanol and finally dried in a 75 °C vacuum oven for 24 h to obtain the fiber adsorbents.

2.3. Characterization. Field emission scanning electron microscopy (SEM, Shimadzu SSX-550) with energy-dispersive X-ray spectroscopy (EDX) was used to observe the fiber samples. A Nicolet iS50 Fourier transform infrared spectrometer was applied to record the Fourier-transform infrared (FTIR) spectra of the samples. X-ray photoelectron spectroscopy (XPS) measurements were tested on a Thermo ESCALAB 250 spectrometer with a Mg-Kα (1253.6 eV) achromatic X-ray source. X-ray diffraction (XRD) patterns were recorded on a Rigaku SmartLab X-ray diffractometer with a Cu-Kα radiation of $\lambda = 1.5418 \text{ \AA}$ (40 kV, 30 mA). N₂ adsorption–desorption isotherms were analyzed by a Quantachrome Autosorb iQ SN analyzer at –196 °C.

2.4. Iodine Adsorption Measurements. **2.4.1. Aqueous Phase Uptake Studies.** To monitor the kinetic adsorption curves of the materials, fibers (20 mg) were added to 100 mL of saturated I₂ aqueous solution or I₃[–] aqueous solution (50.8 mg of I₂ and 33.2 mg of KI in 100 mL of water) with stirring mildly at room temperature. At specific intervals, solution samples were taken out and recorded the change of the solution concentration by UV–vis spectroscopy. The removal efficiency (*R*) of the adsorbents was calculated using the following equation:

$$R = \frac{C_0 - C_t}{C_0} \times 100\% \quad (1)$$

where C₀ and C_t represent the concentration before and after liquid phase adsorption, respectively.

2.4.2. Adsorption Isotherm Study. The adsorption isotherm was conducted by adding 4 mg of samples into 20 mL of I₃[–] solution with different concentrations. The mixed solution was stirred for 6 h, and

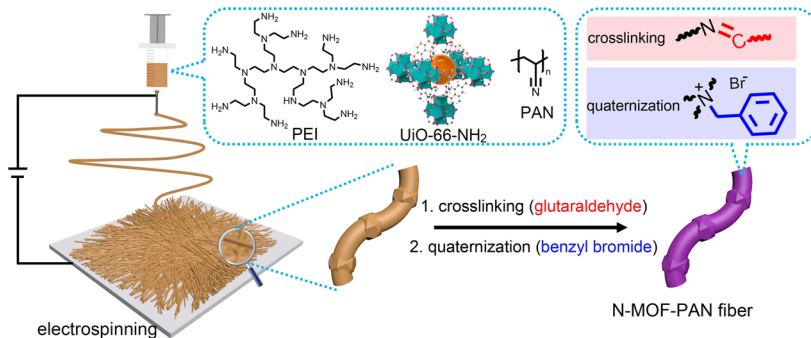


Figure 1. Schematic illustration of the fabrication approach of N-MOF-PAN fibers.

the liquid phase was separated by a filter membrane (nylon-66, 0.22 μm) for iodine concentration determination.

2.4.3. Uptake Capacity for Iodine by the Titration Study. To measure the iodine uptake capacity of the fibers, samples (5 mg) were immersed in an aqueous solution (20 mL) containing 600 mg of KI and 300 mg of I_2 for 24 h with mild stirring.⁶ After this, the residual iodine in the solution was titrated by adding 0.05 M sodium bisulfite aqueous solution using 2% aqueous starch solution as an indicator. Thus, the iodine uptake capacity by the fibers could be calculated.

2.4.4. Adsorption Selectivity Studies. In this study, a certain amount of fiber adsorbents (5 mg) was added into 15 mL of saturated I_2 aqueous solution or I_3^- aqueous solution containing each of various competing anions (SO_4^{2-} , CO_3^{2-} , NO_3^- , CH_3COO^- , and Cl^-) with stirring for 6 h. Fiber adsorbents (5 mg) were also added into 15 mL of saturated I_2 aqueous solution or I_3^- aqueous solution containing various competing anions (SO_4^{2-} , CO_3^{2-} , NO_3^- , CH_3COO^- , and Cl^-) with stirring for 6 h. The concentration of I_2 was 1.2 mM, and the concentration of I_3^- was 1.0 mM. The molar concentration of each competing anion was equal to that of iodine. Afterward, the residual iodine concentration was measured to evaluate the removal efficiency.

2.4.5. pH Value Effect. Fiber adsorbents (5 mg) were added into 15 mL of saturated I_2 aqueous solution or I_3^- aqueous solution with different initial pH values (1–9). The pH values were adjusted with 0.01 M HCl or 0.01 M NaOH solution. After the adsorption for 6 h, the residual iodine concentration was determined.

2.4.6. Reversibility Experiments. For this study, 5 mg of the fibers was immersed in 15 mL of saturated I_2 aqueous solution and I_3^- aqueous solution with stirring slowly. After 6 h of adsorption, the solutions were filtered and tested for concentration measurements. The iodine adsorbed fibers were immersed into ethanol containing 0.1 mol L^{-1} HCl to release iodine, and the regenerated fibers were used for the next adsorption cycle. The cycles were repeated 10 times.

2.4.7. Vapor Phase Capture Studies. The iodine vapor adsorption capacity was evaluated by the gravimetric method. Fiber adsorbents (30 mg) were weighed in diverse vials, which were placed in reaction kettles with iodine particles at the bottom. The sealed containers were exposed at 75 °C until the weight of the materials reached a stable value. During the process of iodine adsorption, the fibers were weighed at certain intervals. The I_2 vapor adsorption capacity of the fibers was obtained from the following formula:

$$M = \frac{m_2 - m_1}{m_1} \times 100\% \quad (2)$$

where M (g g^{-1}) denotes the iodine uptake at time and m_1 and m_2 are the weights of the fibers before and after adsorption of iodine vapor, respectively.

2.4.8. Dynamic Column Adsorption Study. Fiber adsorbents were packed into the adsorption column with a column volume of 2.1 cm^3 . Saturated I_2 aqueous solution was forced through the column with a flow rate of 2 mL min^{-1} by the peristaltic pump. The iodine concentration was monitored during the column adsorption.

3. RESULTS AND DISCUSSION

3.1. Preparation and Characterization of Fiber Materials. As displayed in Figure 1, the synthesis of the composite fibers named N-MOF-PAN fibers integrating N-containing functional groups (cationic quaternary ammonium and uncharged amines) and porous materials (UiO-66-NH₂) was carried out in accordance with the procedures as follows. First, the UiO-66-NH₂ powders were prepared by the classic hydrothermal method (Figure S1). Second, the mixed solution with a polyacrylonitrile (PAN)/polyethyleneimine (PEI)/UiO-66-NH₂ weight ratio of 1:1:1 was electrospun into the precursor fibers. PAN was the polymer support to assist the smooth electrospinning. Finally, after the chemical crosslinking reaction and quaternization reaction, the precursor fibers were converted into N-MOF-PAN fibers. In the crosslinking process, water-soluble PEI was reacted with glutaraldehyde (GA) to make the component PEI water-insoluble. In the quaternization reaction, quaternization reagent benzyl bromide was reacted with the fibers to convert tertiary amine into quaternary ammonium. The preparation processes are simple and easy to produce in a large scale. For comparison, we also prepared the composite fibers only with N-containing functional groups (N-PAN fibers) or only with porous materials (MOF-PAN fibers). Their synthesis processes are shown in the Supporting Information.

The morphology of the obtained fiber materials was observed by the SEM images. As shown in Figure 2, all the

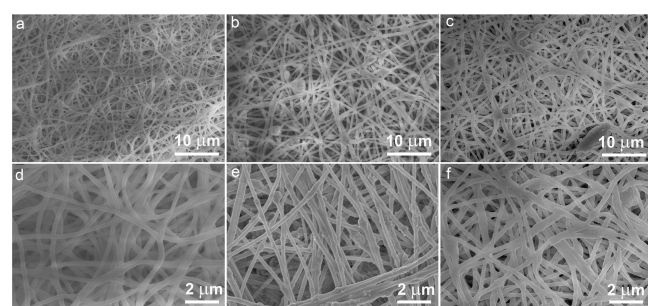


Figure 2. SEM images of N-PAN fibers (a, d), MOF-PAN fibers (b, e), and N-MOF-PAN fibers (c, f).

fibers were continuous with average diameters below 400 nm (Figure S2) and they stacked with each other. Enormous porosity existed among the fibers that could expose more adsorption sites. The surfaces of N-PAN fibers were smooth (Figure 2d); however, obvious hump architectures were located on the surfaces of N-MOF-PAN fibers and MOF-

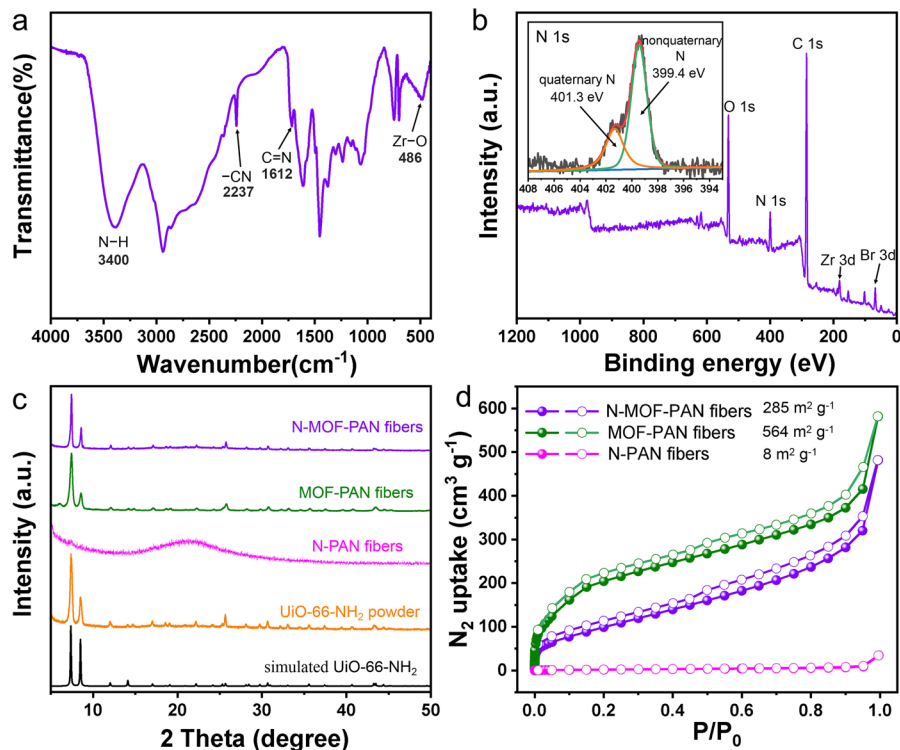


Figure 3. (a) FT-IR spectrum and (b) XPS survey spectrum (the inset is the high-resolution N 1s spectra) of N-MOF-PAN fibers. (c) XRD patterns and (d) N_2 adsorption–desorption isotherms of obtained samples.

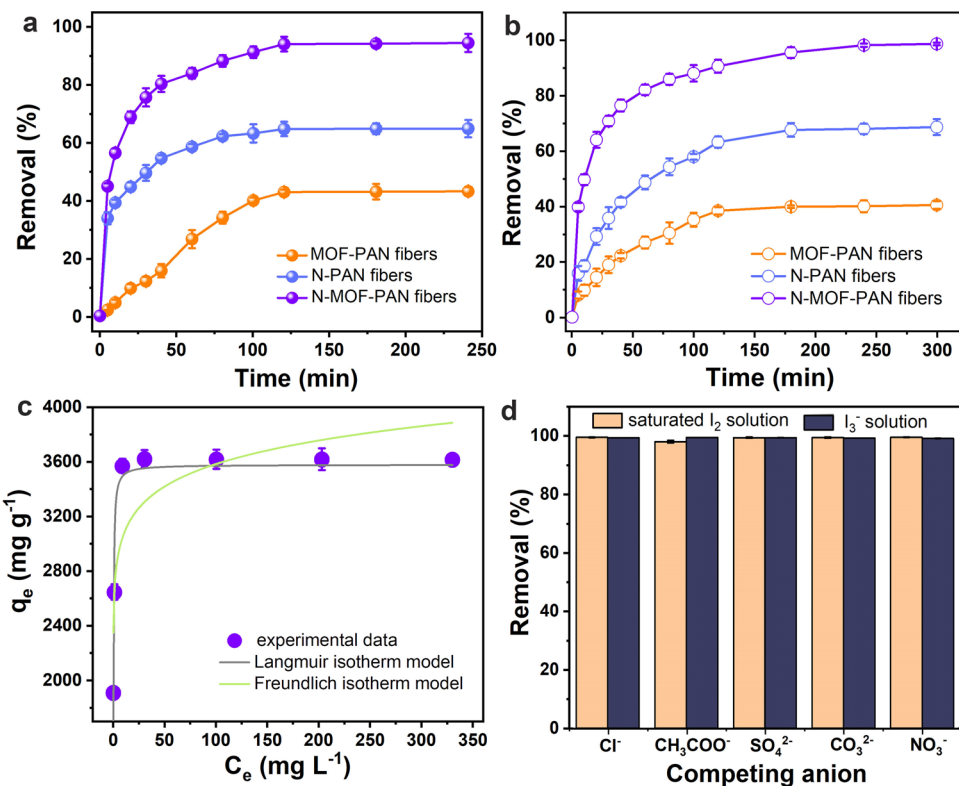


Figure 4. Time-dependent adsorption models for the fibers when contacted with saturated I_2 (a) and I_3^- aqueous solutions (b). Adsorption isotherm of iodine capture from I_3^- aqueous solution by N-MOF-PAN fibers (c). Effect of typical competing anions on the removal percentage of iodine (d).

PAN fibers due to the introduction of $UiO-66-NH_2$ particles (Figure 2e,f). The EDX spectrum from the SEM image of N-MOF-PAN fibers (Figure S3) confirmed their corresponding

elemental composition of C, N, O, Zr, and Br. However, the EDX spectrum for the N-MOF-PAN fibers before quaternization reaction did not display the signal of Br (Figure S4),

suggesting that quaternary ammonium groups are formed after the quaternization reaction. The elemental mapping images revealed that functional groups and MOF particles uniformly distribute in the N-MOF-PAN fibers (Figure S5). The chemical structures of the N-MOF-PAN fibers were studied by FT-IR and XPS spectra. In the FT-IR spectrum of Figure 3a, the peak at 2237 cm^{-1} was the characteristic vibration of $-\text{CN}$ belonging to PAN.³¹ The stretching vibration at 1612 cm^{-1} was attributed to the $\text{C}=\text{N}$ bond, suggesting that the cross-linking reaction happens between the amino groups from PEI in the fibers and aldehyde groups of GA.³² The $\text{N}-\text{H}$ stretching vibration was located at 3400 cm^{-1} .³³ The peak at 486 cm^{-1} corresponded to the $\text{Zr}-\text{O}$ stretching from UiO-66-NH_2 ,³⁴ and this bond was not observed in the FT-IR spectrum of N-PAN fibers (Figure S6) but could be observed in the FT-IR spectrum of MOF-PAN fibers (Figure S7). XPS further verified the elemental composition of N-MOF-PAN fibers that is consistent with the EDX results. What is more, the high-resolution N 1s spectra could be fitted into two peaks at 401.3 and 399.4 eV assigning to cationic quaternary ammonium and uncharged amines, respectively.²⁵ The XPS study was the direct evidence indicating the successful reaction of the quaternization by benzyl bromide. Together with FT-IR results, we can conclude that N-containing functional groups and porous material are introduced into the fibers.

The MOF phase in the composite fibers was further confirmed by the X-ray diffraction (XRD) patterns (Figure 3c). N-PAN fibers were amorphous, agreeing with the previously reported electropun polymer fibers.³⁵ N-MOF-PAN fibers and MOF-PAN fibers had similar diffraction peaks that are well indexed to the peaks of UiO-66-NH_2 powder and the standard simulated XRD pattern from the CIF file of UiO-66-NH_2 , suggesting that the electrospinning process and chemical reactions do not destroy the structures of UiO-66-NH_2 . Nitrogen adsorption–desorption isotherms were carried out to measure the specific surface area, as shown in Figure 3d. Due to the UiO-66-NH_2 component, the Brunauer–Emmett–Teller (BET) surface areas of N-MOF-PAN fibers and MOF-PAN fibers had a significant improvement compared to that of N-PAN fibers ($8\text{ m}^2\text{ g}^{-1}$). The surface area of MOF-PAN fibers ($564\text{ m}^2\text{ g}^{-1}$) was higher than that of N-MOF-PAN fibers ($285\text{ m}^2\text{ g}^{-1}$) because of their more UiO-66-NH_2 content. The high surface area is also beneficial to iodine species capture.

3.2. Iodine Capture from the Aqueous Medium. Based on the above characterization analysis, we then checked the iodine adsorption performance from water by the fiber materials. To verify their wide feasibility for different iodine species in water, saturated I_2 aqueous solution (1.2 mM) and I_3^- aqueous solution (2.0 mM, from mixing KI and I_2) were both served for the adsorption study. Adsorption rate, as a significant index, is crucial to evaluate the performance of adsorbents. Fiber materials (20 mg) were added into 100 mL of I_2 or I_3^- solution to obtain adsorption kinetics. After immersing three kinds of fibers in iodine aqueous solution, the time-dependent UV-vis spectra were studied and the uptake efficiencies of the systems were calculated according to the UV adsorption intensity. As shown in Figure 4a,b, the removal rates for the N-MOF-PAN fibers were higher than those for N-PAN fibers and MOF-PAN fibers. N-MOF-PAN fibers could reach up to 80.0% iodine removal within 50 min, and the equilibrium times were 180 min for saturated I_2 aqueous solution (94.6% removal) and 240 min for I_3^- aqueous solution (98.7% removal). The fast kinetics could guarantee

that N-MOF-PAN fibers are efficient adsorbents. Pseudo-first-order and pseudo-second-order kinetics models were further used to explore the adsorption kinetics data of N-MOF-PAN fibers. As shown in the linear fitting curves (Figure S8) and correlation coefficients (Table S1), the pseudo-second-order kinetics model was more suitable for iodine capture by N-MOF-PAN fibers from both saturated I_2 aqueous solution and I_3^- aqueous solution, suggesting that chemiadsorption processes are involved in the iodine capture.³⁶ The final removal efficiencies of N-MOF-PAN fibers were ~ 1.4 times higher than those of N-PAN fibers and ~ 2.3 times higher than those of MOF-PAN fibers (Figure 4a,b). The results indicated that N-containing functional groups and porous materials synergistically improve the iodine adsorption from water by N-MOF-PAN fibers. Compared with porous materials, N-containing functional groups contributed more to the adsorption. To demonstrate the effect of cationic quaternary ammonium groups, cross-linked PEI/PAN fibers without quaternization were also used to adsorb I_2 or I_3^- (Figure S9). Their adsorption performance was much lower than that of N-PAN fibers, suggesting that cationic quaternary ammonium plays an important role in iodine capture. The color change of the iodine aqueous solution by N-MOF-PAN fiber adsorption was also recorded. The iodine solution changed from dark color to almost colorless during the adsorption (Figures S10 and S11), also suggesting their good removal ability.

The adsorption isotherm of N-MOF-PAN fibers in I_3^- aqueous solution was studied (Figure 4c). The iodine adsorption capacity increased sharply with the increase in the initial iodine concentration and finally tended to be stable due to the full occupation of adsorption sites on the fiber adsorbent. Two classic isotherm models, named Langmuir and Freundlich models, were applied to analyze the equilibrium adsorption data. As observed from the fitting curves (Figure S12) and calculated correlation coefficients (Table S2), the adsorption of iodine on the N-MOF-PAN fibers could be better described by the Langmuir isotherm model and the maximum adsorption capacity calculated by the Langmuir isotherm model could reach 3.61 g g^{-1} , which is superior to other reported adsorbents for iodine adsorption from water (Table S3). In addition, the iodine uptake capacity of N-MOF-PAN fibers was measured in a concentrated KI/I_2 aqueous solution (600 mg of KI and 300 mg of I_2 in 20 mL of H_2O) and the iodine loss in the solution was determined by bisulfite starch titration. The maximum iodine uptake capacity of N-MOF-PAN fibers was found to be as high as 3.56 g g^{-1} , which surpasses most of the reported iodine adsorbents in the aqueous medium (Table S4), further indicating their good iodine adsorption performance from water.

Subsequently, we explored the selectivity of N-MOF-PAN fibers for iodine adsorption, thus providing ideas for the practical application in a complex water system. Sewage generally contains several anions, such as sulfate (SO_4^{2-}), carbonate (CO_3^{2-}), nitrate (NO_3^-), acetate (CH_3COO^-), chloride (Cl^-), etc., which could impede the adsorption of I_2/I_3^- to a certain extent. As shown in Figure 4d, the removal efficiencies toward I_2/I_3^- were still more than 98% when the competing anion was alone in the solution. Moreover, the iodine adsorption efficiencies from saturated I_2 aqueous solution and I_3^- aqueous solution containing multiple competing anions were both larger than 95% (Figure S13). Tap water, lake water, and sea water (lake water was collected

from the Silent Lake in Northeast Normal University, and sea water was collected from the Yellow Sea in Qingdao, China) spiked with iodine were used as the actual samples to evaluate the adsorption performance of N-MOF-PAN fibers (Figure S14). Even in the lake water and sea water with more competitive ions, the removal efficiencies toward I_2/I_3^- could reach up to 80 and 70%, respectively. Therefore, we concluded that plenty of active adsorption sites in the fibers are conducive to the selective capture of iodine. The pH value effect of the iodine solution on the iodine capture was investigated, and the results are displayed in Figure S15. N-MOF-PAN fibers exhibited high iodine removal efficiencies toward I_2/I_3^- in neutral conditions and alkaline conditions. When the solution became acidic, the iodine removal efficiency decreased gradually. At a pH value of 1, due to the competition of abundant Cl^- ions, only 51.7 and 41.1% of iodine were removed from saturated I_2 aqueous solution and I_3^- aqueous solution, respectively. Thus, the iodine adsorption experiments were conducted under neutral conditions in this study.

Furthermore, adsorption/desorption experiments of the N-MOF-PAN fibers were conducted in the liquid phase to determine the reversible process of iodine uptake, which is related to the recovery and utilization of radioactive pollutants. Generally, organic solvents were used to desorb iodine from the iodine-loaded adsorbents.^{8,24} In this study, ethanol and methanol were ineffective for iodine desorption from the iodine-loaded N-MOF-PAN fibers (Figure S16), further demonstrating the strong interactions between the iodine and the fibers. Thus, the N-MOF-PAN fibers could act as an effective iodine storage material. The pH value effect study indicated that N-MOF-PAN fibers have low adsorption capacity for iodine under acidic conditions. Thus, the desorption process was performed by using the elution of ethanol containing 0.1 mol L⁻¹ HCl and the desorption efficiency was more than 99% (Figure S16). After 10 regeneration cycles, the iodine removal was almost unaffected and still maintained relatively excellent adsorption efficiency as high as 95% (Figure S17). The SEM images of N-MOF-PAN fibers after the multi-cycle adsorption are shown in Figure S18. The fibers became swollen and adhesive. However, they still maintained the fiber morphology. The results indicated that the fiber adsorbents possess good stability and recyclability.

3.3. Iodine Capture from the Vapor. Furthermore, the iodine vapor capture of the fiber materials was investigated at 75 °C and ambient pressure. As shown in Figure 5a, the iodine vapor capture capacities had a similar tendency as the iodine adsorption in the aqueous medium and the iodine vapor capture could reach the equilibrium within 8 h. The capture capacities were 3.20 g g⁻¹ for N-MOF-PAN fibers, 2.03 g g⁻¹ for N-PAN fibers, and 1.13 g g⁻¹ for MOF-PAN fibers. Simultaneously, we proved that the iodine vapor capture on the N-MOF-PAN fibers is a reversible process. The captured iodine could be removed from the material when the iodine-loaded material was placed into an acidic alcohol solution (inset in Figure 5b). It should be noted that the N-MOF-PAN fibers still performed a relatively high uptake capacity even after five times reusing (Figure 5b).

3.4. Adsorption Mechanism. The iodine capture mechanism from water by N-MOF-PAN fibers was investigated by means of instrumental analysis. The XRD patterns of N-MOF-PAN fibers after iodine adsorption from saturated I_2 aqueous solution and I_3^- aqueous solution did not exhibit the characteristic diffraction peaks belonging to crystalline I_2 ,⁶

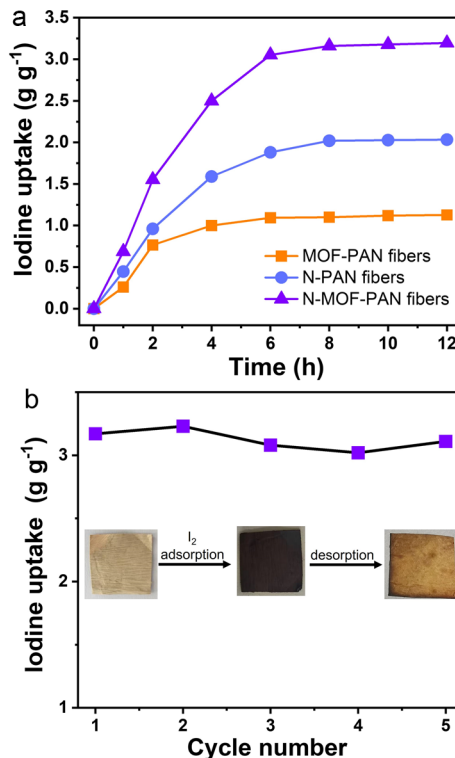


Figure 5. (a) Static adsorption performance of iodine vapor for three kinds of fibers as a function of time at 75 °C and ambient pressure. (b) Plot of iodine vapor uptake efficiency for N-MOF-PAN fibers recorded after five consecutive regeneration cycles (inset: the photographs reflect the color change of the N-MOF-PAN fibers after iodine capture and iodine desorption).

suggesting that other amorphous iodine species are loaded on the fibers (Figure 6a). Furthermore, the survey XPS spectra of N-MOF-PAN fibers after iodine adsorption displayed obvious I 3d peaks (Figure 6b) and these peaks could be resolved into four peaks (Figure 6c). The peaks at 629.7 eV (I 3d_{3/2}) and 618.2 eV (I 3d_{5/2}) were attributed to I_3^- , and the others at 631.4, 631.6 (I 3d_{3/2}), and 620.0 eV (I 3d_{5/2}) were assigned to I_5^- ,³ revealing that chemisorption occurs during the iodine adsorption processes owing to the charge transfer interaction and the forming of charge-transfer complexes.^{4,6,7} In the fibers, N species and benzene rings could act as the effective electron donors.¹¹ Due to these electron-transfer interactions, I_2 was converted to I_3^- and I_3^- was converted to I_5^- . The corresponding compositions based on peak area indicated that I_3^- is the main iodine species in the fiber adsorbents. The amine groups not only provided the electron for polyiodide formation but also offered the charge-transfer complexes. In addition to uncharged amine groups, according to the adsorption capacity comparison (Figure 4a,b), cationic quaternary ammonium groups also adsorbed iodine through Coulomb interactions driving the ion-exchange process from Br^- to polyiodides. This process could be verified by the absence of the Br 3d signal in the survey XPS spectra of iodine-loaded N-MOF-PAN fibers (Figure 6b). The high-resolution N 1s spectra after iodine adsorption were further analyzed. Compared with the original curves (Figure 3b), new peaks appeared at 400.6 and 400.9 eV (Figure 6d) belonging to the N—I bond, indicating the charge-transfer complex formation between amine groups and captured iodine. Additionally, the peaks assigning to cationic quaternary ammonium and

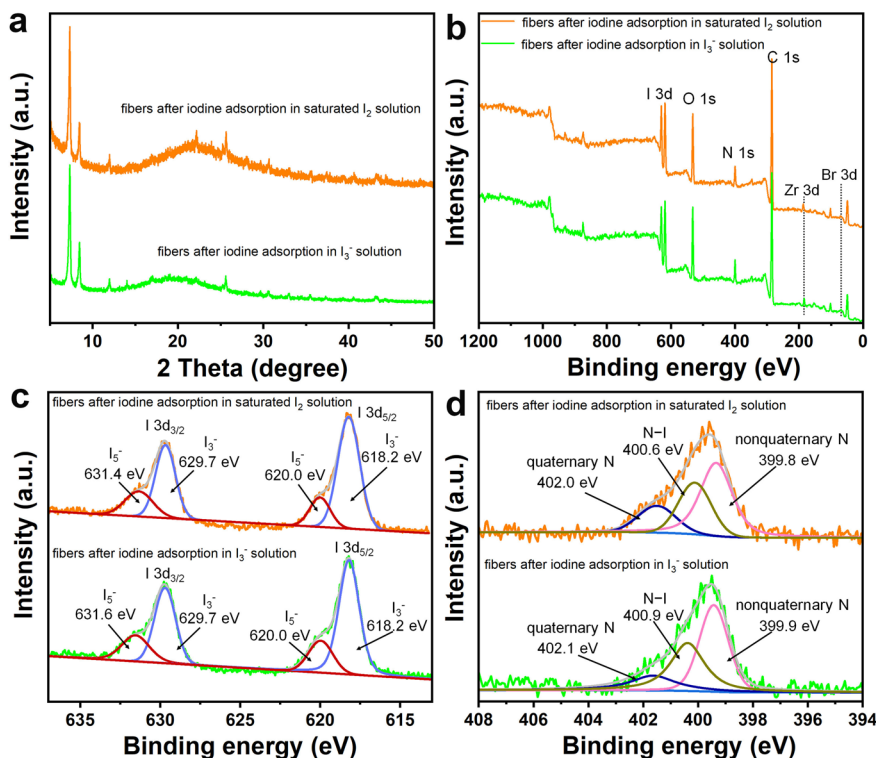


Figure 6. (a) XRD patterns, (b) XPS survey spectra, (c) high-resolution I 3d spectra, and (d) high-resolution N 1s spectra of N-MOF-PAN fibers after iodine adsorption from water.

uncharged amines shifted to higher binding energies, which is the direct evidence of the participation of these adsorption sites in iodine capture. The pore capture mechanism of porous materials during iodine adsorption was confirmed by the BET analysis. The specific surface area of N-MOF-PAN fibers after the iodine capture decreased to $29 \text{ m}^2 \text{ g}^{-1}$ (Figure S19). Based on the above discussion, the overall iodine adsorption process from the aqueous medium by N-MOF-PAN fibers can be demonstrated as follows (Figure 7). I_2 and I_3^- were physically

synergistically led to the good iodine capture performance from water.

3.5. Dynamic Column Adsorption from Saturated I_2 Solution.

The high adsorption capacity, fast kinetics, and macroscopic fiber morphology encouraged us to conduct the dynamic column breakthrough experiments, which are closer to the practical field application (Figure 8a). The N-MOF-PAN fibers (180 mg) were packed in a plastic column with a column volume of 2.1 cm^3 , and saturated I_2 aqueous solution was pumped into the N-MOF-PAN fiber adsorption column with a flow rate of 2 mL min^{-1} . As displayed in Video S1 (Supporting Information), the orange I_2 aqueous solution became colorless when it flowed through N-MOF-PAN fibers, indicating their excellent dynamic I_2 capture capacity from water. We defined a C/C_0 value of 0.05 corresponding to 95% removal as the breakthrough point. As the breakthrough curves shown in Figure 8b, the breakthrough volume for N-MOF-PAN fibers was 1490 mL. After that, the iodine concentration in the filtrate increased gradually because of the decreasing trend of available sites. By stark contrast, the breakthrough volume for commercial activated carbons (ACs) was only 498 mL under the same conditions, again suggesting the high adsorption affinity of N-MOF-PAN fibers toward iodine in water. Moreover, the N-MOF-PAN fibers after the column adsorption process could be also regenerated by 0.1 mol L^{-1} HCl (Figure S20a). The regenerated N-MOF-PAN fibers were used for the repeated column adsorption experiment, and the breakthrough volume was still 1487 mL (Figure S20b), demonstrating their practical application potential.

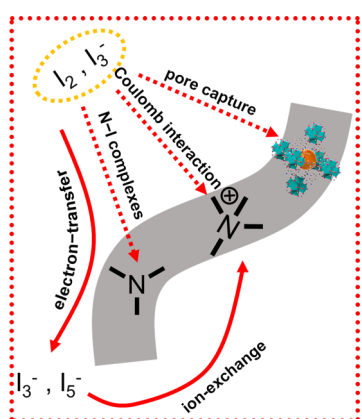


Figure 7. Schematic diagram of a possible adsorption process.

adsorbed on the fibers through Coulomb interaction and pore capture. Simultaneously, chemisorption happened, which produces the polyiodides and forms the charge-transfer complexes. Subsequently, the generated polyiodides were further loaded on the fibers via the ion-exchange process. Thus, the constructed cationic quaternary ammonium groups, uncharged amine groups, and porous materials in the fibers

4. CONCLUSIONS

In summary, we designed and synthesized a novel and easy-to-construct electrospun fiber adsorbent integrating cationic

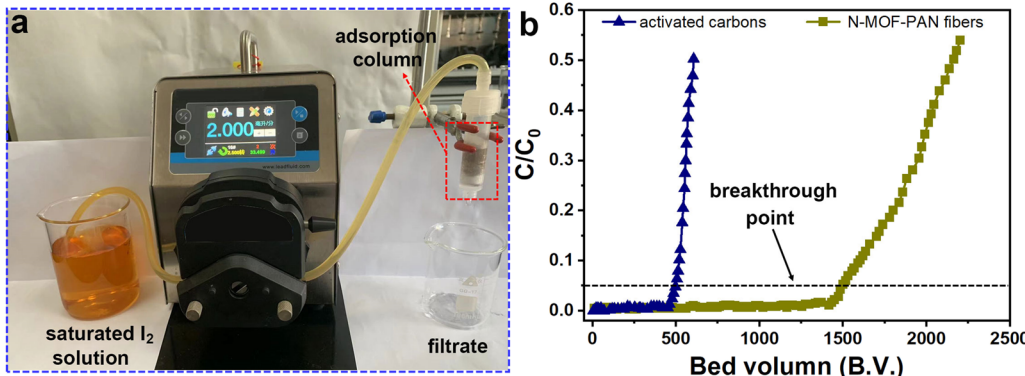


Figure 8. (a) Image of the dynamic column adsorption experimental facility and (b) iodine removal by the N-MOF-PAN fiber packed fixed-bed column from saturated I₂ aqueous solution.

quaternary ammonium groups, uncharged amine groups, and porous material UiO-66-NH₂ that possess high iodine adsorption capacity from the aqueous medium (up to 3.5 g g⁻¹) and fast kinetics (reached equilibrium in 180 min for saturated I₂ aqueous solution and 240 min for I₃⁻ aqueous solution). The high efficiency performance for iodine capture was attributed to the synergistic effect of constructed binding sites. Meanwhile, the present fiber adsorbent manifested attractive selectivity even in the actual water samples and it also showed satisfying recyclability. Different from the reported porous materials as iodine adsorbents, the N-MOF-PAN fibers with macroscopic structures could be efficient column adsorbents with a bed volume of 1490 mL in the dynamic removal test. We thus conclude that the N-MOF-PAN fibers play a crucial role for iodine capture in practical nuclear wastewater remediation, laying the foundation for future studies along these lines.

ASSOCIATED CONTENT

Supporting Information

The Supporting Information is available free of charge at <https://pubs.acs.org/doi/10.1021/acsami.2c14724>.

Material preparation, SEM image of UiO-66-NH₂ powders, diameter distribution, EDX spectra, elemental mapping profile, FT-IR spectra, kinetics fitting plots, kinetics parameters, iodine adsorption by cross-linked PEI/PAN fibers without quaternization, color changes during the iodine adsorption, isotherm fitting plots, isotherm fitting parameters, comparison of iodine adsorption capacities, iodine removal from solution containing multiple competing anions, iodine adsorption in actual water samples, effect of the pH value on the adsorption, desorption kinetics, multi-cycle adsorption of iodine, SEM images after the adsorption, N₂ adsorption-desorption isotherms of N-MOF-PAN fibers after the iodine adsorption, elution process, and repeated column adsorption (PDF)

Dynamic iodine removal by column adsorption (AVI)

AUTHOR INFORMATION

Corresponding Author

Rui Zhao — Key Laboratory of Polyoxometalate and Reticular Material Chemistry of Ministry of Education, Faculty of Chemistry, Northeast Normal University, Changchun

130024, China; orcid.org/0000-0002-2909-8561;
Email: zhaor814@nenu.edu.cn

Authors

Dingyang Chen — Key Laboratory of Polyoxometalate and Reticular Material Chemistry of Ministry of Education, Faculty of Chemistry, Northeast Normal University, Changchun 130024, China

Tingting Ma — Key Laboratory of Polyoxometalate and Reticular Material Chemistry of Ministry of Education, Faculty of Chemistry, Northeast Normal University, Changchun 130024, China

Xinyue Zhao — Key Laboratory of Polyoxometalate and Reticular Material Chemistry of Ministry of Education, Faculty of Chemistry, Northeast Normal University, Changchun 130024, China

Xiaofei Jing — Key Laboratory of Polyoxometalate and Reticular Material Chemistry of Ministry of Education, Faculty of Chemistry, Northeast Normal University, Changchun 130024, China; orcid.org/0000-0002-2289-8355

Guangshan Zhu — Key Laboratory of Polyoxometalate and Reticular Material Chemistry of Ministry of Education, Faculty of Chemistry, Northeast Normal University, Changchun 130024, China; orcid.org/0000-0002-5794-3822

Complete contact information is available at: <https://pubs.acs.org/10.1021/acsami.2c14724>

Author Contributions

[#]D.C. and T.M. contributed equally to this work.

Notes

The authors declare no competing financial interest.

ACKNOWLEDGMENTS

This work was financially supported by the National Natural Science Foundation of China (52003040 and 22131004), Science and Technology Research Project of Education Department of Jilin Province (JJKH20211281KJ), Natural Science Foundation of Department of Science and Technology of Jilin Province (YDZJ202101ZYTS060), and the “111” project (B18012).

REFERENCES

- (1) Liu, C.; Hsu, C. P.; Xie, J.; Zhao, J.; Wu, T.; Wang, H.; Liu, W.; Zhang, J.; Chu, S.; Cui, Y. Half-wave Rectified Alternating Current

- Electrochemical Method for Uranium Extraction from Seawater. *Nat. Energy* **2017**, *2*, 17007.
- (2) Abney, C. W.; Mayes, R. T.; Saito, T.; Dai, S. Materials for the Recovery of Uranium from Seawater. *Chem. Rev.* **2017**, *117*, 13935–14013.
- (3) Luo, D.; He, Y.; Tian, J.; Sessler, J. L.; Chi, X. Reversible Iodine Capture by Nonporous Adaptive Crystals of a Bipyridine Cage. *J. Am. Chem. Soc.* **2022**, *144*, 113–117.
- (4) Zhang, Y.; He, L.; Pan, T.; Xie, J.; Wu, F.; Dong, X.; Wang, X.; Chen, L.; Gong, S.; Liu, W.; Kang, L.; Chen, J.; Chen, L.; Chen, L.; Han, Y.; Wang, S. Superior Iodine Uptake Capacity Enabled by an Open Metal-Sulfide Framework Composed of Three Types of Active Sites. *CCS Chem.* **2022**, *1*.
- (5) Li, B.; Dong, X.; Wang, H.; Ma, D.; Tan, K.; Jensen, S.; Deibert, B. J.; Butler, J.; Cure, J.; Shi, Z.; Thonhauser, T.; Chabal, Y. J.; Han, Y.; Li, J. Capture of Organic Iodides from Nuclear Waste by Metal-Organic Framework-Based Molecular Traps. *Nat. Commun.* **2017**, *8*, 485.
- (6) Xie, L.; Zheng, Z.; Lin, Q.; Zhou, H.; Ji, X.; Sessler, J. L.; Wang, H. Calix(4) pyrrole-based Crosslinked Polymer Networks for Highly Effective Iodine Adsorption from Water. *Angew. Chem., Int. Ed.* **2021**, *60*, 2–10.
- (7) Sen, A.; Sharma, S.; Dutta, S.; Shirodkar, M. M.; Dam, G. K.; Let, S.; Ghosh, S. K. Functionalized Ionic Porous Organic Polymers Exhibiting High Iodine Uptake from Both the Vapor and Aqueous Medium. *ACS Appl. Mater. Interfaces* **2021**, *13*, 34188–34196.
- (8) Chen, R.; Hu, T.; Li, Y. Stable Nitrogen-Containing Covalent Organic Framework as Porous Adsorbent for Effective Iodine Capture from Water. *React. Funct. Polym.* **2021**, *159*, No. 104806.
- (9) Long, X.; Chen, Y. S.; Zheng, Q.; Xie, X. X.; Tang, H.; Jiang, L. P.; Jiang, J. T.; Qiu, J. H. Removal of Iodine from Aqueous Solution by PVDF/ZIF-8 Nanocomposite Membranes. *Sep. Purif. Technol.* **2020**, *238*, No. 116488.
- (10) Tian, Z.; Chee, T. S.; Zhang, X.; Lei, L.; Xiao, C. Novel Bismuth-Based Electrospinning Materials for Highly Efficient Capture of Radioiodine. *Chem. Eng. J.* **2021**, *412*, No. 128687.
- (11) Zhang, Z.; Dong, X.; Yin, J.; Li, Z. G.; Li, X.; Zhang, D.; Pan, T.; Lei, Q.; Liu, X.; Xie, Y.; Shui, F.; Li, J.; Yi, M.; Yuan, J.; You, Z.; Zhang, L.; Chang, J.; Zhang, H.; Li, W.; Fang, Q.; Li, Q.; Bu, X. H.; Han, Y. Chemically Stable Guanidinium Covalent Organic Framework for the Efficient Capture of Low-Concentration Iodine at High Temperatures. *J. Am. Chem. Soc.* **2022**, *144*, 6821–6829.
- (12) Yan, Z.; Yuan, Y.; Tian, Y.; Zhang, D.; Zhu, G. Highly Efficient Enrichment of Volatile Iodine by Charged Porous Aromatic Frameworks with Three Sorption Sites. *Angew. Chem., Int. Ed.* **2015**, *54*, 12733–12737.
- (13) Xie, W.; Cui, D.; Zhang, S. R.; Xu, Y. H.; Jiang, D. L. Iodine Capture in Porous Organic Polymers and Metal-Organic Frameworks Materials. *Mater. Horiz.* **2019**, *6*, 1571–1595.
- (14) Du, H.; Xie, Y.; Zhang, H.; Chima, A.; Tao, M.; Zhang, W. Oxadiazole-Functionalized Fibers for Selective Adsorption of Hg^{2+} . *Ind. Eng. Chem. Res.* **2020**, *59*, 13333–13342.
- (15) Wang, D.; Song, J.; Wen, J.; Yuan, W.; Liu, Z.; Lin, S.; Wang, H.; Wang, H.; Zhao, S.; Zhao, X.; Fang, M.; Lei, M.; Li, B.; Wang, N.; Wang, X.; Wu, H. Significantly Enhanced Uranium Extraction from Seawater with Mass Produced Fully Amidoximated Nanofiber Adsorbent. *Adv. Energy Mater.* **2018**, *8*, 1802607.
- (16) Xue, J.; Wu, T.; Dai, Y.; Xia, Y. Electrospinning and Electrospun Nanofibers: Methods, Materials, and Applications. *Chem. Rev.* **2019**, *119*, 5298–5415.
- (17) Shan, H.; Si, Y.; Yu, J.; Ding, B. Facile Access to Highly Flexible and Mesoporous Structured Silica Fibrous Membranes for Tetracyclines Removal. *Chem. Eng. J.* **2021**, *417*, No. 129211.
- (18) Zhao, R.; Chen, D.; Gao, N.; Yuan, Y.; Hu, W.; Cui, F.; Tian, Y.; Shi, W.; Ma, S.; Zhu, G. Porous Cationic Electrospun Fibers with Sufficient Adsorption Sites for Effective and Continuous $^{99}TcO_4^-$ Uptake. *Adv. Funct. Mater.* **2022**, *32*, 2200618.
- (19) Li, W.; Li, Y.; Wen, X.; Teng, Y.; Wang, L.; Yang, T.; Li, X.; Li, L.; Wang, C. Flexible Zr-MOF Anchored Polymer Nanofiber Membrane for Efficient Removal of Creatinine in Uremic Toxins. *J. Membr. Sci.* **2022**, *648*, No. 120369.
- (20) Yu, M.; Guo, Y.; Wang, X.; Zhu, H.; Li, W.; Zhou, J. Lignin-Based Electrospinning Nanofibers for Reversible Iodine Capture and Potential Applications. *Int. J. Biol. Macromol.* **2022**, *208*, 782–793.
- (21) Gogia, A.; Das, P.; Mandal, S. K. Tunable Strategies Involving Flexibility and Angularity of Dual Linkers for a 3D Metal-Organic Framework Capable of Multimedia Iodine Capture. *ACS Appl. Mater. Interfaces* **2020**, *12*, 46107–46118.
- (22) He, D.; Jiang, L.; Yuan, K.; Zhang, J.; Zhang, J.; Fan, Q.; Liu, H.; Song, S. Synthesis and Study of low-Cost Nitrogen-Rich Porous Organic Polyaminals for Efficient Adsorption of Iodine and Organic Dye. *Chem. Eng. J.* **2022**, *446*, No. 137119.
- (23) Hijazi, A.; Azambre, B.; Finqueneisel, G.; Vibert, F.; Blin, J. L. High Iodine Adsorption by Polyethyleneimine Impregnated Nano-silica Sorbents. *Micropor. Mesopor. Mater.* **2019**, *288*, No. 109586.
- (24) Ai, C.; Feng, J.; Yang, S.; Xiong, S.; Tang, J.; Yu, G.; Pan, C. Enhanced Iodine Capture by Incorporating Anionic Phosphate Unit into Porous Networks. *Sep. Purif. Technol.* **2021**, *279*, No. 119799.
- (25) Xie, Y.; Pan, T.; Lei, Q.; Chen, C.; Dong, X.; Yuan, Y.; Shen, J.; Cai, Y.; Zhou, C.; Pinna, I.; Han, Y. Ionic Functionalization of Multivariate Covalent Organic Frameworks to Achieve an Exceptionally High Iodine-Capture Capacity. *Angew. Chem., Int. Ed.* **2021**, *60*, 22432–22440.
- (26) Zhao, R.; Tian, Y.; Li, S.; Ma, T.; Lei, H.; Zhu, G. An Electrospun Fiber Based Metal-Organic Framework Composite Membrane for Fast, Continuous, and Simultaneous Removal of Insoluble and Soluble Contaminants from Water. *J. Mater. Chem. A* **2019**, *7*, 22559–22570.
- (27) Hao, S.; Wen, J.; Li, S.; Wang, J.; Jia, Z. Preparation of COF-LZU1/PAN Membranes by an Evaporation/Casting Method for Separation of Dyes. *J. Mater. Sci.* **2020**, *55*, 14817–14828.
- (28) Uliana, A. A.; Bui, N. T.; Kamcev, J.; Taylor, M. K.; Urban, J. J.; Long, J. R. Ion-Capture Electrodialysis Using Multifunctional Adsorptive Membranes. *Science* **2021**, *372*, 296–299.
- (29) Ding, L.; Shao, P.; Luo, Y.; Yin, X.; Yu, S.; Fang, L.; Yang, L.; Yang, J.; Luo, X. Functionalization of UiO-66-NH₂ with Rhodanine via Amidation: Toward a Robust Adsorbent with Dual Coordination Sites for Selective Capture of Ag(I) from Wastewater. *Chem. Eng. J.* **2020**, *382*, No. 123009.
- (30) Li, X.; Zhang, B.; Tang, L.; Goh, T.; Qi, S.; Volkov, A.; Pei, Y.; Qi, Z.; Tsung, C. K.; Stanley, L.; Huang, W. Cooperative Multifunctional Catalysts for Nitrene Synthesis: Platinum Nano-clusters in Amine-Functionalized Metal-Organic Frameworks. *Angew. Chem., Int. Ed.* **2017**, *56*, 16371–16375.
- (31) Zhao, R.; Shi, X.; Ma, T.; Rong, H.; Wang, Z.; Cui, F.; Zhu, G.; Wang, C. Constructing Mesoporous Adsorption Channels and MOF-Polymer Interfaces in Electrospun Composite Fibers for Effective Removal of Emerging Organic Contaminants. *ACS Appl. Mater. Interfaces* **2021**, *13*, 755–764.
- (32) Wang, S.; Xiao, K.; Mo, Y.; Yang, B.; Vincent, T.; Faur, C.; Guibal, E. Selenium (VI) and Copper (II) Adsorption Using Polyethyleneimine-Based Resins: Effect of Glutaraldehyde Cross-linking and Storage Condition. *J. Hazard. Mater.* **2020**, *386*, No. 121637.
- (33) Zhao, R.; Li, X.; Sun, B.; Li, Y.; Li, Y.; Yang, R.; Wang, C. Branched Polyethyleneimine Grafted Electrospun Polyacrylonitrile Fiber Membrane: A Novel and Effective Adsorbent for Cr (VI) Remediation in Wastewater. *J. Mater. Chem. A* **2017**, *5*, 1133–1144.
- (34) Tripathy, S. P.; Subudhi, S.; Das, S.; Ghosh, M. K.; Das, M.; Acharya, R.; Acharya, R.; Parida, K. Hydrolytically Stable Citrate Capped Fe₃O₄@UiO-66-NH₂ MOF: A Hetero-Structure Composite with Enhanced Activity towards Cr (VI) Adsorption and Photo-catalytic H₂ Evolution. *J. Colloid Interface Sci.* **2022**, *606*, 353–366.
- (35) Zhang, C.; Li, X.; Bian, X.; Zheng, T.; Wang, C. Polyacrylonitrile/Manganese Acetate Composite Nanofibers and Their Catalysis Performance on Chromium (VI) Reduction by Oxalic Acid. *J. Hazard. Mater.* **2012**, *229–230*, 439–445.

- (36) Zhao, R.; Li, X.; Li, Y.; Li, Y.; Sun, B.; Zhang, N.; Chao, S. C.; Wang, C. Functionalized Magnetic Iron Oxide/Polyacrylonitrile Composite Electrospun Fibers as Effective Chromium (VI) Adsorbents for Water Purification. *J. Colloid Interfaces Sci.* **2017**, *505*, 1018–1030.

□ Recommended by ACS

Sodium Alginate-Based Carbon Aerogel-Supported ZIF-8-Derived Porous Carbon as an Effective Adsorbent for Methane Gas

Mengge Shang, Serguei Filatov, *et al.*

MARCH 13, 2023

ACS APPLIED MATERIALS & INTERFACES

READ ↗

Smart Solvent-Responsive Covalent Organic Framework Membranes with Self-regulating Pore Size

Ziye Song, Jianguo Liu, *et al.*

MARCH 17, 2023

ACS APPLIED POLYMER MATERIALS

READ ↗

Decoration of Cauliflower-Like TiO₂ on Nanofibrous PVDF Membranes: A Strategy for Wastewater Treatment

Fayez U. Ahmed and Debarun Dhar Purkayastha

FEBRUARY 01, 2023

ACS APPLIED POLYMER MATERIALS

READ ↗

Silver/Graphene Nanocomposite as an Additive for Aqueous Lubrication

Lupeng Wu, Weiwei Shi, *et al.*

JANUARY 25, 2023

ACS APPLIED NANO MATERIALS

READ ↗

[Get More Suggestions >](#)